Astron. Astrophys. 326, 1215–1227 (1997)

ASTRONOMY AND ASTROPHYSICS

Physical association between the Southern Coalsack and the Chamaeleon-Musca dark clouds⋆

W.J.B. Corradi[1,2], **G.A.P. Franco**[1], **and J. Knude**[2]

[1] Departamento de Física – ICEx – UFMG, Caixa Postal 702, 30161-970, Belo Horizonte – MG, Brazil
[2] Niels Bohr Institute for Astronomy, Physics and Geophysics, Juliane Maries Vej 30, DK-2100, Copenhagen Ø, Denmark
(corradi@astro.ku.dk, franco@fisica.ufmg.br, indus@astro.ku.dk)

Received 20 August 1996 / Accepted 5 June 1997

Abstract. The results of a photometric programme aiming to investigate the hypothesis of a physical association between the Southern Coalsack and the Chamaeleon-Musca dark clouds are presented. The analysis is based upon $uvby\beta$ photometry for 1017 stars selected from the Smithsonian Astrophysical Observatory star catalog to cover these clouds and the connecting area defined by the galactic coordinates: $308^\circ \geq l \geq 294^\circ$ and $-20^\circ \leq b \leq 5^\circ$. To ensure a more complete sample the data were complemented by $uvby\beta$ photometry for 213 stars of Kapteyn's Selected Area 203, that lies at the center of the Chamaeleon-Musca dark clouds complex.

The distribution of the colour excesses $E(b-y)$ for stars with line-of-sight *inside* and *outside* the dark clouds' contours indicates the presence of a local low absorption volume that is limited at 150 ± 30 pc from the Sun by an extended interstellar dust feature, and is followed by another region with almost no additional reddening for another 350 pc. Combined with other data on the local ISM, the existence of the dust feature permeating the whole connecting area and the identical distance of the Southern Coalsack and Chamaeleon-Musca dark clouds suggest that these clouds could be dense condensations in the diffuse medium composing the interface of the Local and Loop I Bubbles.

Apparently, the minimum column density of the dust feature does not show a clear dependence with the galactic longitude, but may increase with the galactic latitude in the sense that $[E(b-y)_{\rm min}, b] = [0\overset{\rm m}{.}050; 0^\circ] \rightarrow [0\overset{\rm m}{.}100; -8^\circ] \rightarrow [0\overset{\rm m}{.}150; -15^\circ]$. The quoted increase suggests either the approaching of the tangential point of a warped sheet-like structure of same column density and curved away from the Sun, or an inhomogeneous sheet-like structure roughly perpendicular to the galactic plane.

Key words: stars: distances – ISM: clouds – ISM: individual objects: Southern Coalsack – Chamaeleon-Musca – Loop I – Local Bubble

1. Introduction

Accurate distances to dark clouds and their distribution in the Interstellar Medium (ISM) are important tools that can provide constraints for studies of, e.g., star formation, infrared emission, ultraviolet scattering and shadowing experiments. The Southern Coalsack and the Chamaeleon-Musca dark clouds have been subject of various investigations, but the results have been disagreeing (Franco 1989a, 1991; Schwartz 1991).

The Southern Coalsack (l = 303°, b = 0°) has a complex structure and in some places shows several velocity components (Nyman et al. 1989). Although highly fragmented, a characteristic of clouds with star formation, it seems to be one of the few massive (3500 $M_\odot$) molecular clouds without star formation (e.g. Westerlund 1960; Tapia 1973; Weaver 1973; Bok et al. 1977). A distance of 150 pc was first suggested by Unsöld (1929) and Müller (1934) by means of star count studies. Later, Rodgers (1960) determined a value of 174 pc from photographic photometry. Seidensticker (1987, 1989), using UBV and Hβ photoelectric photometry, proposed that the Southern Coalsack was mainly composed by two clouds, respectively, 188 and 243 pc from the Sun.

Franco (1989a) used Strömgren $uvby\beta$ photometry and found that the cloud might be at 180 ± 26 pc. Recently, analysing colour excesses from a fainter magnitude limited sample towards Selected Area 194 (SA 194), which covers the northern part of the cloud, Franco (1995) has found that the main structure of the Southern Coalsack is not farther than 200 pc from the Sun, with indications of dust as close as 150 pc.

The Chamaeleon-Musca complex is mainly formed by four clouds: Cha I (l = 297.°2, b = −15.°6), Cha II (l = 303.°0, b = −14.°3), Cha III (l = 302.°4, b = −17.°4) and Musca

Send offprint requests to: W.J.B. Corradi (Brazilian Address)

⋆ Based on data collected with the Strömgren Automatic Telescope - SAT - Danish 50 cm installed at the European Southern Observatory (ESO) in La Silla, Chile

(l = 300.°6, b = −8.°5). The distance to Cha I is the most discussed, not only due to difficulties in obtaining a consistent explanation for the extinction law towards the cloud, but also because of the interest on it as a region of rich low-mass star formation. Most attempts to obtain the distance to Cha I has been centered on the analysis of the very young star HD 97300, which is clearly associated to this cloud (Cederblad 1946). The discussion has been whether the ratio R of total to selective extinction is abnormal ($R \approx 5$) or not ($R \approx 3$). If R is normal an explanation of the infrared excess observed for this star is missing (Henize 1963; Grasdalen et al. 1975; Hyland et al. 1982; Jones et al. 1985; Thé et al. 1986; Steenman & Thé 1989). Distances ranging from 115 to 215 pc have been suggested. Independently of this star, a distance estimate to Cha I was proposed by Whittet et al. (1987), who derived a distance of 140 pc using a colour excess vs. distance relation for field stars. This value implies an anomalous extinction law toward HD 97300.

Concerning the distance to the other clouds very little has been done so far. According to King et al. (1979), Cha II would be between 165 and 330 pc. Hetem et al. (1988) proposed a distance of 200–250 pc to Musca assuming that it was possibly related to the Chamaeleon complex. Fitzgerald et al. (1976) investigating the Thumbprint nebula, close to the line-of-sight of Cha III, suggested a distance of 400 pc to this nebula. Graham & Hartigan (1988) assumed this distance as being the most appropriate to Cha II.

Using $uvby\beta$ photometry for stars in SA 203, which lies close to the geometrical center of the Chamaeleon-Musca complex but without covering most of the complex's clouds, Franco (1991) suggested the existence of a sheet-like structure positioned at about 140 pc. It was also suggested that the clouds in this general direction could be physically associated, forming an extended structure. If so, Cha I is placed at 140 pc, in agreement with Whittet et al. (1987), and Cha II would be no farther than 158 ± 40 pc, much closer than the otherwise suggested 400 pc.

1.1. Are the Southern Coalsack and the Chamaeleon-Musca dark clouds physically associated?

With a standard value for R = 3.1, a comparison of the colour excess $E(b-y)$ vs. distance diagrams for the Chamaeleon-Musca complex (Franco 1991) and the Southern Coalsack (Franco 1989a) shows great similarities. As can be seen in Fig. 1, the jump of the colour excess to higher values occurs approximately at the same distance, and the observed minimum value of this rise is almost the same: $\Delta E(b-y) \approx 0.^{\rm m}100$.

Although the clouds are apart by more than 15° these facts suggest that they might be dense condensations embedded in an extended interstellar structure. As discussed in this paper, such a structure might be related to the interface between the Local and Loop I Bubbles.

The observational data are described in Sect. 2 and colour excesses vs. distance diagrams are used in Sect. 3 to investigate the reddening distribution. The two low reddening volumes and the sheet-like dust feature are discussed in connection to the other data on the local ISM in Sects. 4 and 5, respectively. The conclusions are summarized in Sect. 6.

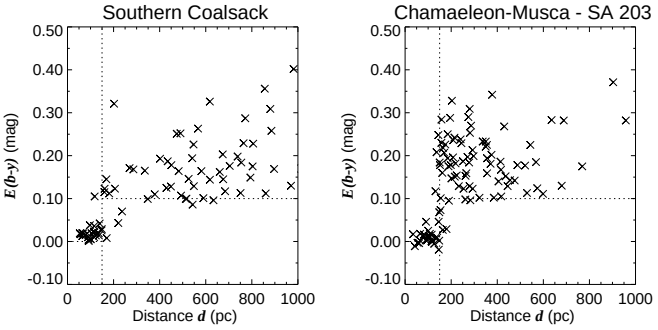

Fig. 1. Colour excess vs. distance diagrams, obtained by Franco (1989a, 1991), for the stars covering the Southern Coalsack and the Chamaeleon-Musca clouds. Besides the clouds are apart from each other by more than 15° both diagrams show similar characteristics. A standard value (R = 3.1) has been adopted for the extinction law

2. Observational data

In order to sustain the hypothesis of a physical association of the Southern Coalsack and the Chamaeleon-Musca complex, a new photometric programme has been carried out to trace the extinction between the features. We used the Strömgren Automatic Telescope (SAT) in La Silla, Chile, to obtain $uvby\beta$ photometry for all stars in the area defined by the galactic coordinates 308° ≥ l ≥ 294° and −20° ≤ b ≤ 5°, that were earlier than G0 in the catalog of the Smithsonian Astrophysical Observatory (SAO).

The SAT is equipped with a permanent six-channel $uvby\beta$ spectrograph-photometer (Florentin-Nielsen 1985), which allows simultaneous four-colour measurements for the $uvby$ passbands, or simultaneous measurements for the narrow and wide passbands used to define the Hβ index. Most stars were observed at least four times, twice in $uvby$ and twice in Hβ. These measurements were used to obtain the visual photoeletric V magnitude, the colour index $(b-y)$, the colour index differences m_1 and c_1, and the Hβ index on the standard system (Crawford & Barnes 1970; Grønbech et al. 1976; Crawford & Mander 1966).

The rms errors for one observation of one star are $0.^{\rm m}008$, $0.^{\rm m}004$, $0.^{\rm m}006$, $0.^{\rm m}009$ and $0.^{\rm m}011$, in V, $(b-y)$, m_1, c_1 and β, respectively. Details describing the observational method and the data for the 1017 observed stars can be found in Corradi & Franco (1995). The data were complemented by the $uvby$ and Hβ measurements of 213 stars from the Potsdam Spektral-Durchmusterung of the SA 203, at the geometrical center of the Chamaeleon-Musca dark clouds (Franco 1992).

Intrinsic colours, absolute magnitudes and distances have been computed following the calibrations suggested by Crawford (1975, 1978, 1979) and Olsen (1988). For the F-type stars the calibration of Olsen (1988) was adopted instead of Crawford (1975) since the former includes metal weak stars. The accuracy of reddenings and distances is estimated by the propagation of

Table 1. Galactic delineation of the eight sub-areas, and their respective total number of stars N

Sub-area	Gal. Longitude $l\,(^\circ)$	Gal. Latitude $b\,(^\circ)$	N
I	$308 \geq l \geq 300$	$0 \leq b \leq +5$	118
II	$300 \geq l \geq 294$	$0 \leq b \leq +5$	88
III	$308 \geq l \geq 300$	$-5 \leq b \leq 0$	45
IV	$300 \geq l \geq 294$	$-5 \leq b \leq 0$	61
V	$308 \geq l \geq 300$	$-12 \leq b \leq -5$	54
VI	$300 \geq l \geq 294$	$-12 \leq b \leq -5$	46
VII	$308 \geq l \geq 300$	$-20 \leq b \leq -12$	49
VIII	$300 \geq l \geq 294$	$-20 \leq b \leq -12$	49

the measuring errors into the calibrations, applying the method described by Knude (1978a). Taking into account the rms errors of one observation of one star, stated above, colour excesses $E(b-y)$ have been estimated with a mean accuracy of $0\overset{\mathrm{m}}{.}018$, and the distances to the A- and F-type stars with mean accuracy of 21%. For the B-type stars the distance accuracy is within 15–30%. To calculate stellar distances standard ratio between visual absorption and reddening $A_V = 4.3\,E(b-y)$ has been adopted.

In order to compute intrinsic properties a set of criteria must be met. The criteria are those proposed by Olsen (1979), Crawford (1975, 1978, 1979) and Tobin (1985); and a detailed description is given by Franco (1989b). Known variables were also excluded (Kholopov et al. 1985), e.g. LZ Cen (Vaz et al. 1995), as well as stars with mean errors larger than 5 times the standard deviation in any magnitude and/or colour indices. Moreover, as the estimates of $E(b-y)$ and distance for stars belonging to the intermediate group, mostly composed by A1-A2 type stars, may be less accurate they were also excluded from the present analysis.

Of the 1218 stars, only 510 fulfilled the imposed selection criteria. The (l, b) positions of the final sample of accepted stars are given in Fig. 2. The thick contours are the lowest opacity level of the photographic Dark Clouds Catalogue (DCC) compiled by Feitzinger & Stüwe (1984). The thinner contour is the outer 2 K km s^{-1} velocity integrated CO emission for the Southern Coalsack (Nyman et al. 1989). The horizontal and vertical dashed lines delineate eight sub-areas that will be used to discuss the details of the reddening distribution. The limits of the sub-areas, identified by the roman numbers, are summarized in Table 1.

Stars with line-of-sight *inside* and *outside* the DCC contours, are indicated by the ($\times$) and (+) signs, respectively. Such a division seems proper for our analysis of a connection between the diffuse and dense ISM. Near the galactic plane ($-5^\circ \leq b \leq 5^\circ$) the DCC contours may be partially related to some background clouds that are not associated to the Southern Coalsack, so a sub-group *inside* the CO contour has been defined to avoid this problem. Stars in this sub-group are indicated by the ($\square$) signs.

The last column of Table 1 indicates the total number of stars in each sub-area. The average number of stars per square degree

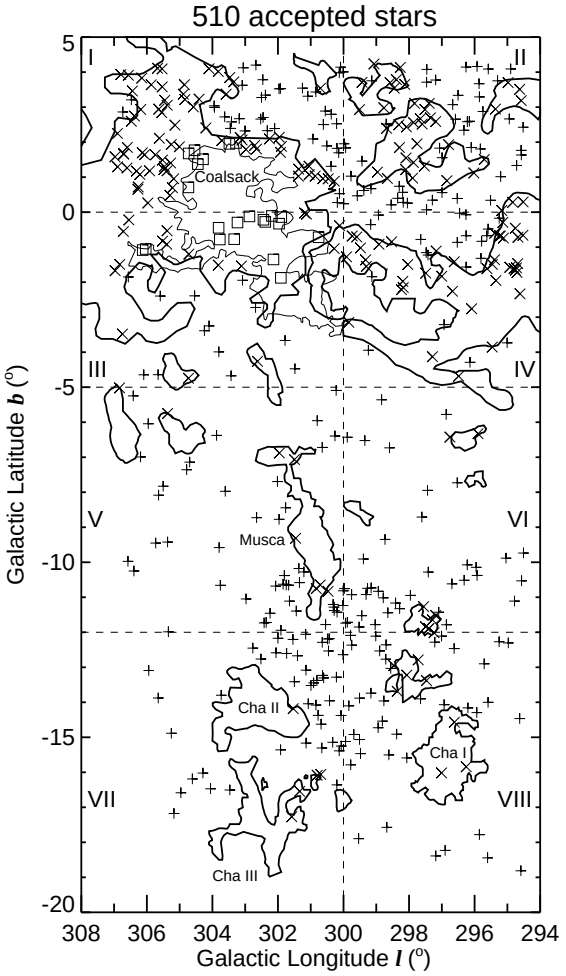

Fig. 2. Distribution of the 510 stars which fulfilled the imposed selection criteria. The clouds' contours defined by the thick lines are the lowest opacity level of the DCC and the thin one is the outer 2 K km s^{-1} velocity integrated CO emission contour for the Southern Coalsack. Stars with line-of-sight *inside* and *outside* the DCC contours are represented by the ($\times$) and (+) signs, respectively. Stars *inside* the CO contour are indicated by the ($\square$) signs. The horizontal and vertical dashed lines delineate eight sub-areas identified by roman numbers

ranges from 0.8 to 3. This variation is probably of no importance since we are probing a large scale feature. We are aware that the stellar magnitude distribution over the field is inhomogeneous, but since a lower reddening envelope is the interesting issue the varying limiting magnitude carries no importance. The working hypothesis is that a sheet is present from the Coalsack to the Chamaeleon-Musca dark clouds and, where we have a star beyond ≈ 150 pc, the sheet is detected. The feature is coherent - Fig. 1 shows that beyond 150 pc no zero reddening stars are present - so all stars must be affected by a common structure.

3. Reddening distributions

With the colour excesses and distances of the 510 selected stars $E(b-y)$ vs. d(pc) diagrams have been obtained. Figs. 3a and

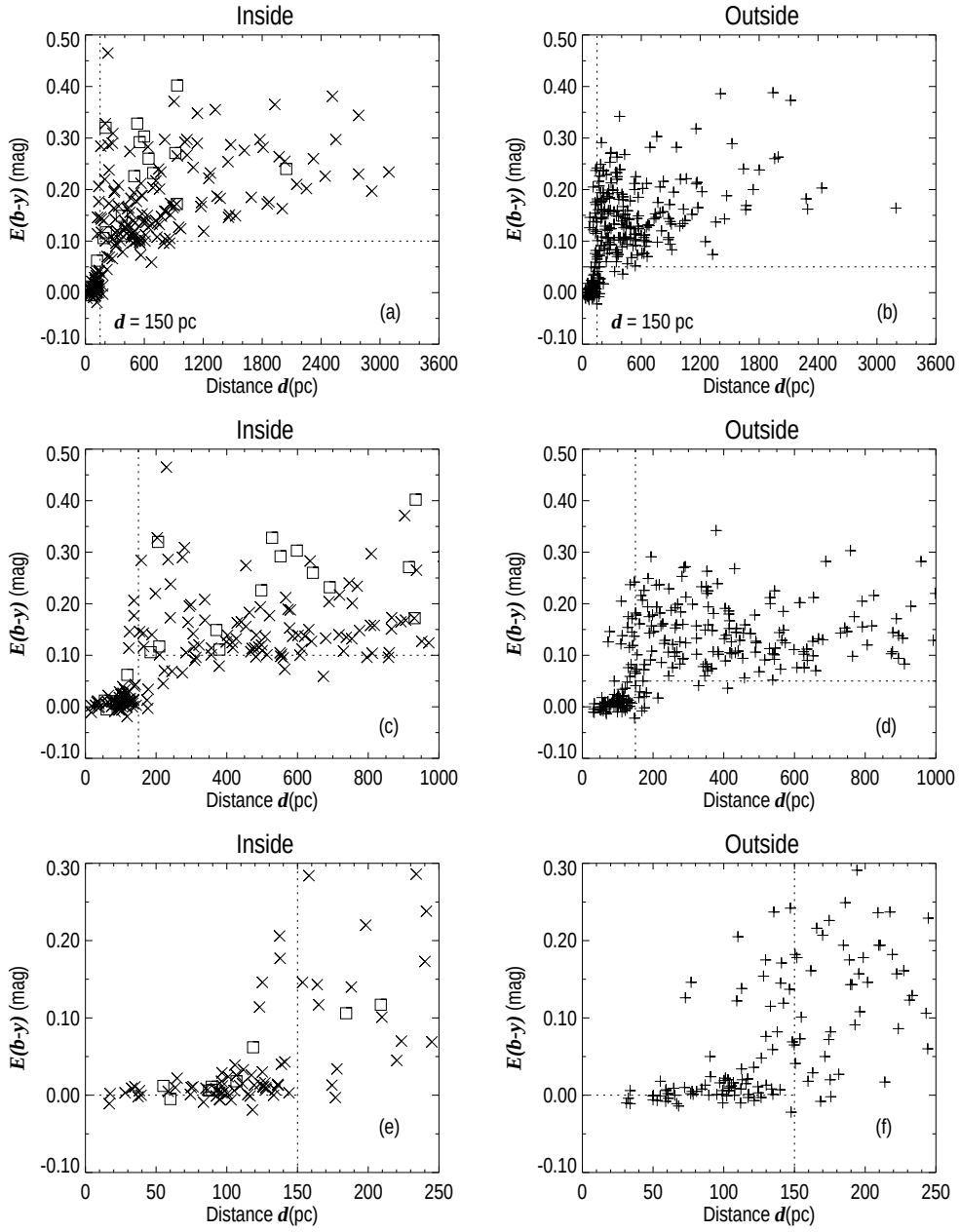

Fig. 3a–f. Colour excess vs. distance diagrams for the accepted stars. **a** in the *inside* group. **b** in the *outside* group. The vertical dotted lines at d = 150 pc indicate where higher absorption sets in and the horizontal ones indicate the respective lower envelopes of absorption $E(b-y) \approx 0\overset{\mathrm{m}}{.}100$ (*inside*) and $E(b-y) \approx 0\overset{\mathrm{m}}{.}050$ (*outside*) formed beyond this distance. Stars in the sub-group *inside* the CO emission contour for the Southern Coalsack (□ signs) have the same behaviour of the other *inside* stars. **c and d** detailed view up to distances of 1 kpc, where the lower envelopes can be better seen, suggesting that an extended interstellar structure has probably been crossed. **e and f** detailed view up to 250 pc. The foreground reddening is very low to both groups and a transition region, where $E(b-y)$ has a sudden increase, sets in the distance range of 150 ± 30 pc

3b show a region up to about 150 pc with very little reddening, which is followed by another region with a lower envelope $E(b-y) \approx 0\overset{\mathrm{m}}{.}100$ to the *inside* and $E(b-y) \approx 0\overset{\mathrm{m}}{.}050$ to the *outside* groups. The vertical dotted lines at d = 150 pc indicate where higher absorption sets in and the horizontal ones indicate the respective lower envelopes of absorption formed beyond this distance.

Figs. 3c and 3d are a view for distances up to 1 kpc. The lower envelopes of minimum reddening can be better seen, suggesting that an extended interstellar structure may have been crossed. Note that stars *inside* the CO contour follow the tendency of the others *inside* the DCC contours. An even more detailed view up to 250 pc can be seen in Figs. 3e and 3f. The foreground reddening is very low to both *inside* and *outside* groups, and, at the distance range of 150 ± 30 pc, a transition region appears where the $E(b-y)$ values have a sudden increase.

The $E(b-y)$ vs. d diagrams of the eight sub-areas, up to distances of 1 kpc, are shown in Fig. 4 to the *inside* (*left*) and *outside* (*right*) groups. The structure in all sub-areas is fairly similar, i.e., there is a steep rise of the reddening after 150 ± 30 pc forming a lower envelope of minimum absorption beyond this distance. Note also the presence of an upper envelope of maximum absorption. These effects indicate that an extended interstellar structure can be permeating the whole area.

Since the observed stars are within different dark clouds the colour excesses, shown in Fig. 3, could be either the effect of a common structure containing the embedded molecular clouds or just an effect of different superposing structures. In order to investigate how the reddening is distributed over the area

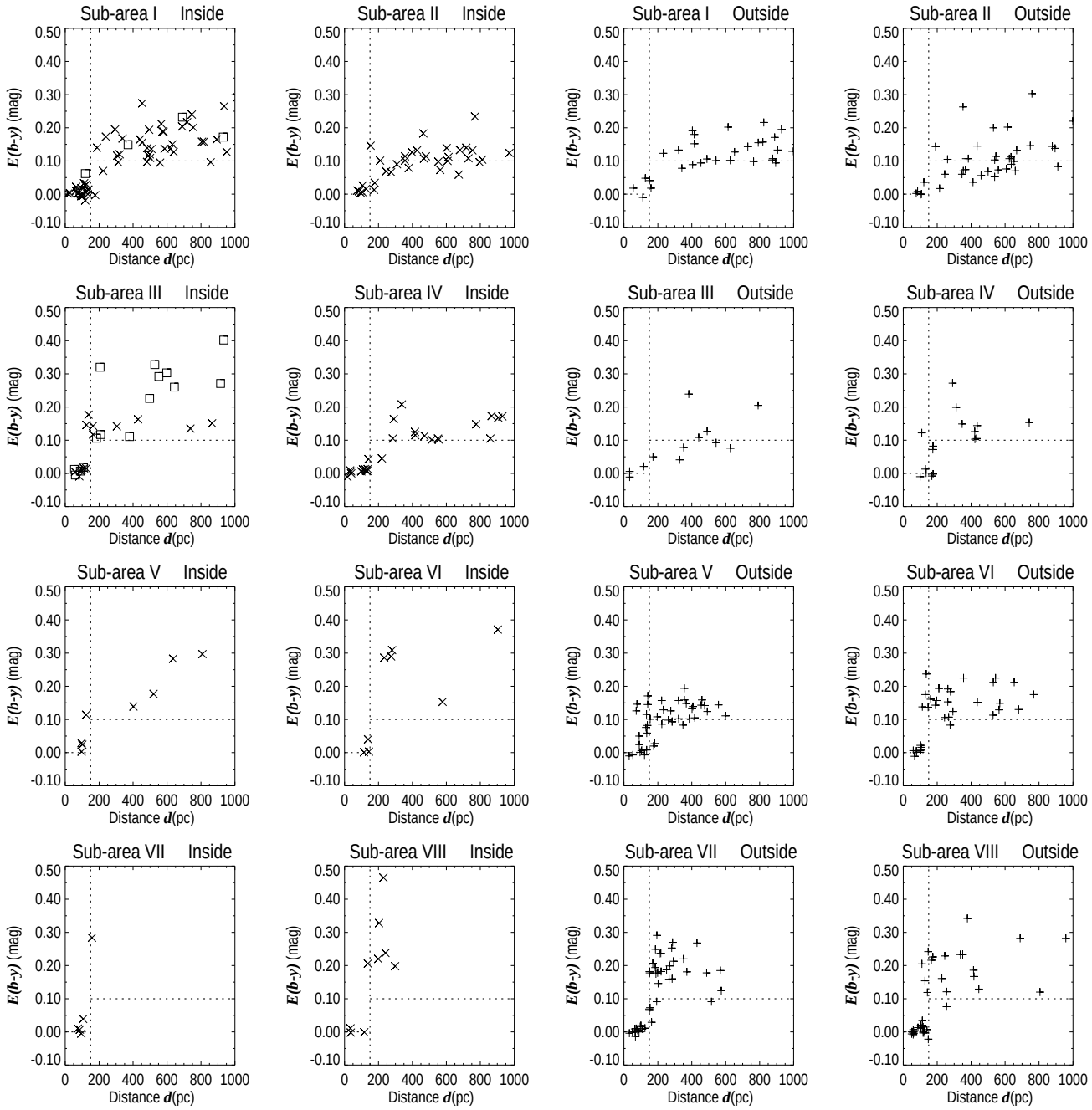

Fig. 4. $E(b-y)$ vs. d diagrams for the eight sub-areas investigated, up to distances of 1 kpc. (*left*) to the *inside* group. (*right*) to the *outside* group. The structure in all sub-areas is fairly similar with the steep rise of the reddening, after 150 $\pm$ 30 pc, forming a lower envelope of minimum absorption beyond this distance. Such effect indicates the existence of a structure permeating the whole area. Note, however, that the lower envelope of colour excesses seems to be increasing its minimum value with the galactic latitude, as can be visualized using the reference dashed lines (see discussion in the text)

we have analysed the colour excesses using the eight sub-areas mentioned on Sect. 2.

It is remarkable that the lower envelope of colour excesses seems to have an increasing value with galactic latitude, as can be visualized using the reference dashed lines traced at $E(b-y)$ = $0\overset{\mathrm{m}}{.}100$. For the *outside* group, near the galactic plane, but mostly in sub-area II, the lower envelope of $E(b-y)$ seems to be around $0\overset{\mathrm{m}}{.}050$. Increases to around $0\overset{\mathrm{m}}{.}100$ in sub-areas V-VI, and seems to further increase to $0\overset{\mathrm{m}}{.}150$ in sub-area VII.

For the *inside* group a similar effect may be present, but the small number of stars at the higher latitudes does not allow such an increasing effect to be clearly revealed. Anyway, near the galactic plane the lower level seems to be $0\overset{\mathrm{m}}{.}100$, then increases to around $0\overset{\mathrm{m}}{.}150$ in sub-areas V-VI, and most proba-

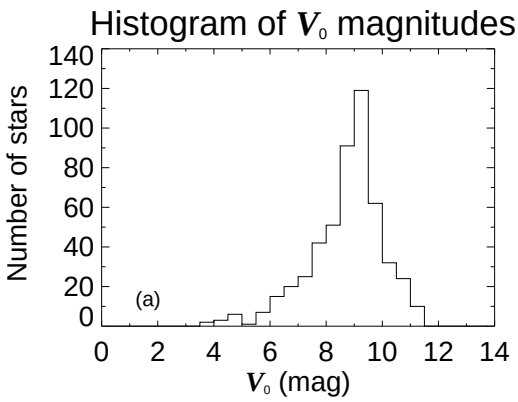

Fig. 5. a Histogram of photoeletric V_0 magnitudes for the 510 stars fulfilling the selection criteria. Note the decrease in the number of stars fainter than $V_0 \approx 9\overset{m}{.}5$ meaning that (for SAO and Potsdam stars) the final sample may be complete, in magnitude, only down to this value

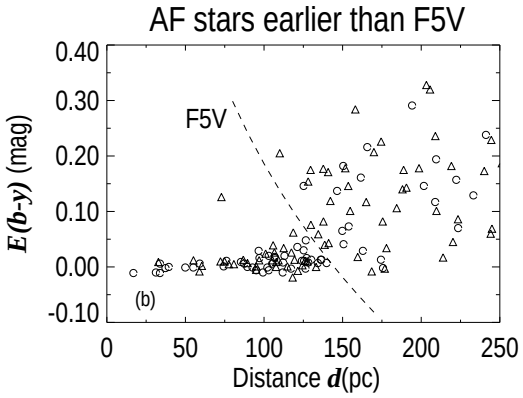

Fig. 5. b Colour excess vs. distance diagram for the subsample of A- and F-type stars earlier than F5 V. The (△) represents the A-type stars and the (○) the F-type. The dashed curve is the maximum observable $E(b-y)$ for a zero age main sequence F5 V star with magnitude $V_0 = 9\overset{m}{.}5$. Note that stars showing additional reddening of $E(b-y) = 0\overset{m}{.}1 - 0\overset{m}{.}3$ would still be included in the sample within 100 pc

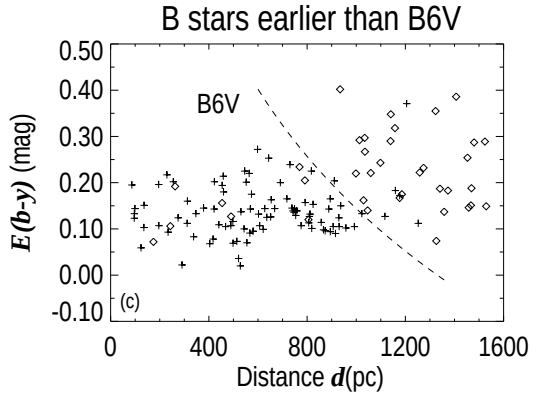

Fig. 5. c Same as 5b, but for all B-type stars earlier than B6 V. The stars in the range B6 V - B3 V are represented by (+) and those earlier than B3V, by (◇). The dashed curve has the same meaning, but for a zero age main sequence B6 V star. With the B-type stars being able to pick up larger colour excesses even at greater distances, no reddenings larger than those observed seem to exist

bly increases to $0\overset{m}{.}200$ in sub-areas VII-VIII. In sub-area II for the *inside* and *outside* groups the envelope is remarkably well defined at $0\overset{m}{.}050$. There are some stars indicating this value as a minimum reddening for sub-areas I, III and IV, which might suggest $E(b-y) \approx 0\overset{m}{.}050$ as representative of the reddening caused by the feature's most diffuse parts. We refer to Sect. 4 for a more thorough discussion.

Summing up, the existence of a common envelope of minimum colour excess starting approximately at the same distance in all sub-areas suggests obscuring material distributed in an extended interstellar structure. The Southern Coalsack and the Chamaeleon-Musca dark clouds seem to be part of the sheet since they are also located at 150 ± 30 pc from the Sun. As the complete range of colour excess from $\approx 0\overset{m}{.}100$ to $0\overset{m}{.}275$, shown by the stars in a very narrow distance slot centered on 150 pc (Figs. 3e and 3f), does not change for another 350 pc (Fig. 3c and particularly 3d) the dust sheet at 150 pc may be followed by another low column density volume. Finally, if the increase of the $E(b-y)$ lower envelope's value with the galactic latitude is real, it could be either due to approaching the tangential point of a warped sheet-like structure of same column density and curved away from the Sun, or an inhomogeneous sheet-like structure roughly perpendicular to the galactic plane.

3.1. Limiting magnitude effects on $E(b-y)$ and distances

In a sample of probes from a limited spectral range and brighter than a common faintest magnitude the reddening data are expected to be complete to a maximum observable colour excess, given at each distance by the sample's limiting magnitude, rather than being complete to the distance of the most distant observed star (Knude 1987). The histogram of the V_0 magnitudes for the 510 accepted stars, shown in Fig. 5a, indicates that there is a decrease in the number of stars fainter than $V_0 \approx 9\overset{m}{.}5$, the approximate SAO limit. As our sample may be complete only down to this value, it would be important to see if this limit has any effects on the inclusion of colour excesses.

The colour excess vs. distance diagram in Fig. 5b illustrates that larger colour excesses could have been detected, assuming they existed, by plotting all A- and F-type stars in the restricted spectral/luminosity range earlier than F5 V. The A- and F-type stars are represented by (△) and (○), respectively. The dashed curve indicates the maximum detectable $E(b-y)$ as a function of distance for a zero age main sequence (standard line) F5 V star with magnitude $V_0 = 9\overset{m}{.}5$.

As several stars in this sub-sample are expected to be more luminous than the zero age main sequence F5 V, the dashed curve is a lower limit to the maximum detectable $E(b-y)$ at a given distance, which means that such stars have residual ca-

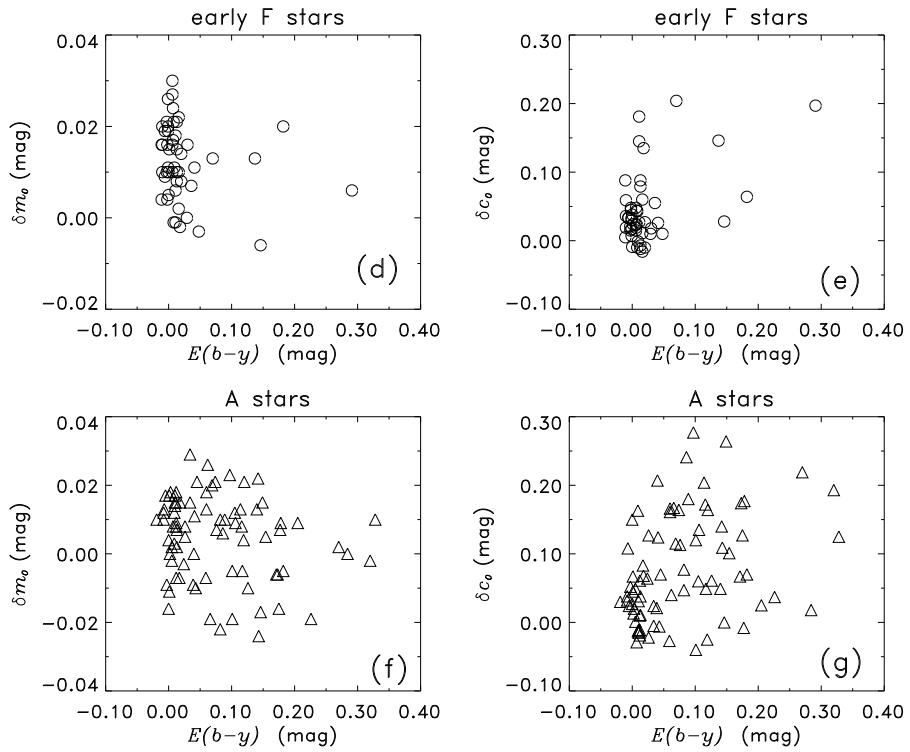

Fig. 5. d δm_o vs. $E(b-y)$, **e** δc_o vs. $E(b-y)$ for all early F-type stars in the sample with magnitude $V_0 \leq 9\overset{\text{m}}{.}5$. **f-g** Same, but for all A-type stars. The existence of a limiting magnitude introduces no correlation between colour excesses and stellar properties. Therefore, the features on the colour excess vs. distance diagrams must be representative, instead of being caused by selection effects

pacity to pick up more reddening. In other words, stars showing additional reddening of $E(b-y) = 0\overset{\text{m}}{.}1 - 0\overset{\text{m}}{.}3$ would still be included in the sample brighter than $V_0 = 9\overset{\text{m}}{.}5$, depending on the distance.

The same discussion can be illustrated for the earliest stars of the sample. The B-type stars are intrinsically brighter and can pick up larger reddenings, even at the larger distances. In Fig. 5c all B-type stars earlier than B6 V were plotted. The dashed curve still have the same meaning, but for a zero age main sequence B6 V star with magnitude $V_0 = 9\overset{\text{m}}{.}5$. Stars in the range B6 V - B3 V are represented by (+), and those earlier than B3 V by ($\diamond$). With the B-type stars being able to pick up larger colour excesses, even at greater distances, no reddenings larger than those observed seem to exist at the covered distance range.

Moreover, the use of a magnitude limited sample of A- and F-type stars to probe a dusty environment may also be the explanation for some relationship between colour excess $E(b-y)$ and stellar properties δm_0, δc_0 (Knude 1991). The photometric parameters δm_0 and δc_0 are correlated to [Fe/H] and how much brighter than the standard line a star is. Because of the sample's limiting magnitude, for a given intrinsic stellar colour the probability to observe less evolved stars decreases with distance, implying that we might be unable to observe most old metal-rich stars at a given distance. Generally, we could say that we would tend to observe only the less reddened ones at large distances.

Figs. 5d-g show the $\delta m_0 - E(b-y)$ and $\delta c_0 - E(b-y)$ diagrams for subsamples of early F-type and A-type stars, with magnitude $V_0 \leq 9\overset{\text{m}}{.}5$. These diagrams do not show any correlation between stellar properties and colour excesses, implying that the existence of a limiting magnitude seemingly does not affect the completeness of the colour excesses and distances entering the final sample. Therefore, we conclude that the features on the colour excess vs. distance diagrams must be representative, instead of being caused by selection effects.

4. The low reddening volumes

4.1. The local low reddening volume and the Local Bubble

In the immediate solar neighbourhood the observational data suggest that the Sun is immersed at the edges of a warm (T $\approx$ 8000 K), low density ($n_{\rm HI} < 0.1$ cm^{-3}) and mostly neutral ($n_{\rm e}/n_{\rm HI} < 0.5$) interstellar cloudlet termed the Local Interstellar Cloud (LIC). The LIC has a maximum neutral hydrogen column density $N_{\rm HI} \approx 2 \times 10^{19}$cm^{-2}, with $N_{\rm HI} \approx 10^{18}$ cm^{-2} being a typical value. It becomes ionized at the farther edges, and, if uniform extends 2-30 pc in some directions (e.g., Bertaux et al. 1985; Bruhweiler & Vidal-Madjar 1987; Frisch et al. 1990; Lallement et al. 1995).

The LIC and other cloudlets are embedded in an irregularly shaped region, whose radius ranges from 30 to 300 pc, and is deficient in dense neutral hydrogen compared to the galactic average (Frisch & York 1983, 1991; Paresce 1984; Snowden et al. 1990; Juda 1991; Welsh et al. 1994; Tinbergen 1982; Warwick et al. 1993; Malina et al. 1994; Perry & Johnston 1982). Usually called Local Bubble, this cavity is filled with hot (T $\approx 10^6$ K), low-density ($n_{\rm HI} \leq 0.025$ cm^{-3}) gas, and as recently shown by the ROSAT and EUVE shadowing experiments, coexists with the neutral atomic and molecular gas within its interior (e.g. Kerp 1993; Snowden et al. 1991, 1993, 1995; Wang & Yu 1995, Bowyer et al. 1995).

The Local Bubble origin has been long discussed by various authors (e.g. Cowie & Songaila 1986; Cox & Reynolds 1987; Bochkarev 1987; Kosarev 1994; Hartquist 1994; Bruhweiler 1996). One interpretation is that the confinement of the Local Bubble could be the edges of a remnant from a supernova (SN) explosion that pressurized and heated the hot gas, swept out, compressed and destroyed the cooler gas within its interior, but was shaped by the existing large scale cool gas (Cowie & Songaila 1986).

It has been suggested either that the Geminga pulsar could be the remnant of such a SN explosion which took place near the Sun less than 1 million years ago (Gehrels & Chen 1993; Frisch 1993) or that the Local Bubble may have been produced around 10^6 years ago by various SN explosions of stars from an already dissolved stellar association (e.g. Hartquist 1994). On the other hand, Bruhweiler (1996) suggested that there may not exist a bubble, with the contours being, in fact, defined by the intersection of the dense neutral gas shock fronts of large interstellar structures, like the Orion-Eridanus Bubble, Gum Nebula and the four radio continuum loops, Loop I to IV.

Since the closest star in our sample is at 15 pc the LIC cannot be addressed properly. Neither it seems appropriate to make generalizations on the Local Bubble exclusively from our data. Nevertheless, one certain conclusion is that a local low absorption volume exists in the general direction surveyed. The stars in the *inside* and *outside* groups show that between 15 and 100 pc from the Sun, the average colour excess is $0\overset{\mathrm{m}}{.}006$ and $0\overset{\mathrm{m}}{.}004$, respectively, with a standard deviation of $\pm\ 0\overset{\mathrm{m}}{.}008$ in both cases. If the standard dust-to-gas relation (Knude 1978b) can be applied, the obtained neutral hydrogen column densities are $N_{\rm HI} = 4.5 \times 10^{19}$ cm^{-2} and $N_{\rm HI} = 3 \times 10^{19}$ cm^{-2}, characteristic of the lowest column densities found in the cold neutral ISM.

Up to 100 pc, the intercloud component of the ISM contributes with $0\overset{\mathrm{m}}{.}002$ and closer than 150 pc less than 50% of the sky is expected to be covered by diffuse interstellar clouds (Knude 1979a, 1983). These clouds have mean colour excess $E_0(b-y) = 0\overset{\mathrm{m}}{.}030$, and an expected number of 4.3 per kpc (Knude 1979b, 1981). Thus, the solar vicinity could be seen as virtually free from dust within 75-100 pc or, instead, as containing 4.4×10^{-4} clouds pc^{-3} filling about 2% of the volume and distributed randomly in a low density medium (Knude 1984a).

This means that average reddenings may not be representative if the matter has a clumped distribution, with a significant amount of material concentrated only in a small part of the sky. Fig. 6a shows a very expanded view of the colour excess vs. distance diagrams for both *inside* and *outside* groups (previously given in Sect. 3) that supports the existence of the local low absorption volume.

As can be seen, the very small values of the colour excesses in both diagrams are spread in the whole distance range, even within 100-120 pc, where the probability to have one cloud is 30-40%, that is, the probability to be unreddened is 60%. In the *inside* diagram, there are 16 stars between 100 and 120 pc, implying 4-5 stars expected to have $E(b-y) \geq 0\overset{\mathrm{m}}{.}030$.

Further support to the existence of a local low reddening volume is given by the spatial distribution of the colour excesses shown in Fig. 6b. The stars are spread over the whole surveyed area, and apart from two very reddened ones, represented by the black squares, most of them present colour excesses lower than $\sigma_{E(b-y)}$, i.e., lower than $0\overset{\mathrm{m}}{.}018$. Among the 65 lines of sight, five stars indicate directions with colour excesses between $\sigma_{E(b-y)}$ and $E_0(b-y)$, and only one between $E_0(b-y)$ and $0\overset{\mathrm{m}}{.}055$ (which corresponds to $\approx 3 \times \sigma_{E(b-y)}$). Note that in some directions, even *inside* the line of sight of the dark molecular clouds, almost no reddening is measured. Based on these diagrams, one would rather suggest that the clouds are randomly distributed in a low density medium, but probably occupying a small fraction of the volume.

The two most reddened stars mentioned above are SAO 252318 (l = 306$\overset{\circ}{.}$4, $b = -5\overset{\circ}{.}3$) and SAO 251863 ($l$ = 300$\overset{\circ}{.}$3, $b = -6\overset{\circ}{.}4$). Both located in sub-area V, they show rather high colour excesses ($0\overset{\mathrm{m}}{.}146$ and $0\overset{\mathrm{m}}{.}126$) at quite short distances of 77 and 73 pc, respectively. Except for the reddening, the photometry seems normal. On the other hand, they have been classified in the Michigan Catalogue (Houck & Cowley 1975) as G0 III and A5 III/IV stars, with remarks, which indicates that one should not be so confident on this spectral classification, and very careful when interpreting the results obtained for these two stars. Despite they met our selection criteria they were excluded from the averaging processes. The acquisition of additional photometry, as well as high dispersion spectroscopy would be interesting in order to investigate the existence or not of dust clouds nearer than 100 pc in these directions.

4.2. The second low reddening volume and Loop I

The Local Bubble is believed to interact with Loop I, another large neighbouring bubble along the whole fourth galactic quadrant. Loop I is centered at $l = (329^\circ \pm 1^\circ)$ and $b = (18^\circ \pm 3^\circ)$, and has a diameter of $116^\circ \pm 4^\circ$ (Berkhuijsen et al. 1971). According to Weaver (1979) strong stellar winds, acting on the material left-over after the Sco-Cen OB association has been formed, created a bubble of gas and dust concentric to the association.

In this picture, Loop I would be a single SN shell produced by the explosion of one of the most massive members of Sco-Cen OB association, having this shell inflated inside the hot, uniform and low density volume of the previously swept up (wind-driven) bubble. Arguing that a single SN remnant model would require different energies of explosion to fit the HI shell, radio continuum loop and X-ray data together, Iwan (1980) proposed that Loop I would be an old SN remnant that would have been reheated by a second SN shock.

In a more recent study de Geus (1992) identified three different HI shells with each one of the sub-groups (proposed by Blaauw 1964) of the Sco-Cen OB association: Upper Centaurus-Lupus (UCL), Upper Scorpius (US) and Lower Centaurus-Crux (LCC). The UCL-shell would be the one modeled by Weaver (1979) and Iwan (1980). It would be located at 140 $\pm$ 20 pc

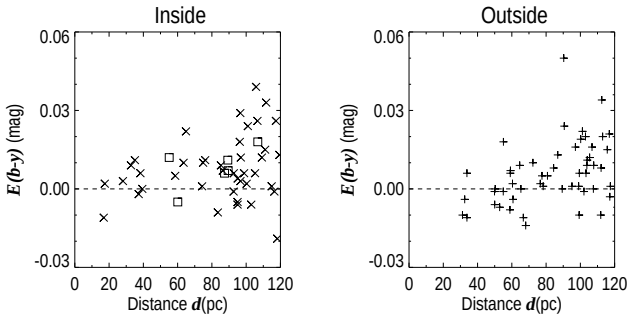

Fig. 6. a Expanded view of the colour excess vs. distance diagrams. (*left*) *inside* group. (*right*) *outside* group. The local volume is characterized by very small values of the colour excesses, even around 100-120 pc where some of the stars should be reddened by, at least, one average diffuse cloud. The two most reddened stars within 120 pc, SA0 251863 and 252318, were not included in the *outside* diagram (cf. Fig. 3f and see text for further comments)

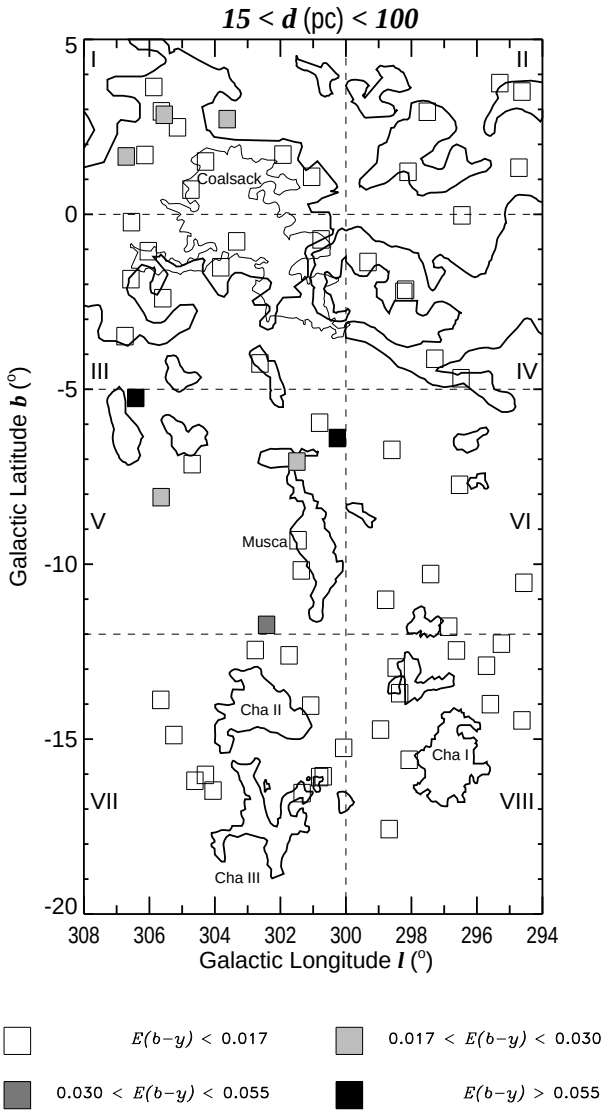

Fig. 6. b Spatial distribution of the colour excesses of the stars nearer than 100 pc. Apart the two very reddened stars (black squares) most of those spread over the whole area present reddening lower than $\sigma_{E(b-y)}$, characterizing the low reddening volume

from the Sun, centered at (l = 320°, b = 10°), and with radius of 110 ± 30 pc.

The US-shell, related to the Ophiuchi complex, would be located at 160 ± 22 pc, with center at (l = 347°, b = 21°) and radius of 40 ± 4 pc. The LCC-shell, besides the coincidence with the LCC sub-group did not show kinematic structure of neutral gas being part of an expanding shell. Nevertheless, from the curvature of the HI loop at (l = 295°, b = 18°), it was deduced that the shell should be located at 130 ± 24 pc from the Sun, with center at (l = 300° ± 5°, b = 8° ± 5°) and radius of 35 ± 10 pc.

The almost constant envelopes of minimum and maximum colour excess, centered in a very narrow distance slot around 150 pc (cf. Figs. 3e and 3f), remain unchanged for about 350 pc after crossing the dust feature suggesting that a second low reddening region has been reached. Such a low density region can be identified with the interior of the Loop I Bubble.

5. The dust sheet-like feature

The effects of the extended absorbing dust feature, that confines the low reddening volume, can be visualized on the diagrams of $E(b-y)$ vs. l (Fig. 7a) and $E(b-y)$ vs. b (Fig. 7b). The dashed lines indicate the limits of the sub-areas, and the stellar distances have been restricted to less than 500 pc. The sheet and the no-reddening values are present - and well separated - everywhere.

In sub-areas I, III and IV the lower envelopes of colour excess around $E(b-y) \approx 0\overset{\text{m}}{.}100$ strongly indicate the influence of the outskirts of the Southern Coalsack on the reddening distribution. The fact that these values are comparable to those obtained for stars with line of sight *inside* the CO contour suggests that the surrounding material is probably related to the cloud, in agreement with what would be expected from the displayed DCC contours. In sub-area VII, which contains the molecular clouds Cha II and Cha III, it seems highly probable that the colour excesses are caused by the front layer of these clouds. In this sub-area, for the longitude range $308° \geq l \geq 303°$, the lack of stars with high colour excesses values is not real, but due to the absence of measured stars (see Fig. 2).

Apparently, the jump in $E(b-y)$ caused by the dust feature does not show clear dependence with the galactic longitude, but may increase with the galactic latitude. If the jump in $E(b-y)$ really increases with the galactic latitude, it could be represented by $[E(b-y)_{\min}, b] = [0\overset{\text{m}}{.}050; 0°] \rightarrow [0\overset{\text{m}}{.}100; -8°] \rightarrow [0\overset{\text{m}}{.}150; -15°]$. The quoted increase might indicate, if we postulate that the dust sheet is roughly perpendicular to the galactic plane, that the sheet does not have the same optical thickness because $E(b-y)_{\min}\,(b)$ does not follow a simple $E(b-y)\sec(b)$ law.

The quoted increase might also be the result of approaching the tangential point of a warped sheet-like structure with same

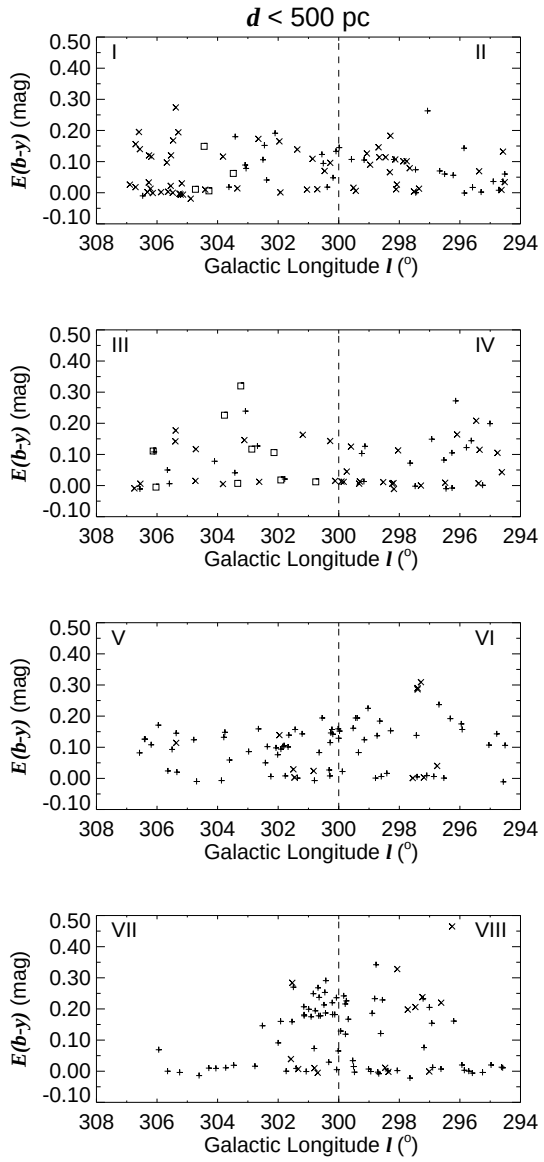

Fig. 7. a $E(b-y)$ vs. l diagrams. The extended interstellar absorbing feature, that covers the whole connecting area, causes a shift to higher values forming lower envelopes of minimum $E(b-y)$ in all eight sub-areas. The value of this shift does not show clear dependence with the galactic longitude, but, as we move to the higher latitudes an increase of the shift can be noted. In sub-area VII, all stars with $l \geq 303^\circ$ are within 150 pc (details in the text)

column density, curved away from the Sun. If the dust sheet is part of a small bubble, it could be associated to the LCC-shell proposed by de Geus (1992). If the dust sheet is part of a larger structure, warped in this part of the sky, it could be associated to the UCL-shell, as proposed by Iwan (1980). Owing to the small surveyed latitude range, we cannot rule out any of the possibilities, but, the reddening data do not show clear signs of the LCC-shell existence. Neither Crawford (1991), using high resolution observations of interstellar Na I and Ca II found positive velocity components corresponding to the receding part of this shell.

Close to the galactic plane, along directions where the DCC higher opacity is not expected, the minimum colour excess is $E(b-y)_{\rm min} \approx 0\overset{\rm m}{.}050$. Some stars in sub-areas I, III and IV, and even most of the stars of the *inside* group in sub-area II suggest that this minimum value should be representative of the diffuse medium constituting the dust sheet in this region of the sky. One could think about the combined column density of $4.3 \times (120 + 350)/1000$ interstellar diffuse clouds, whose $E_0(b-y) = 0\overset{\rm m}{.}030$, were initially occupying the 120 pc of the observed local volume and the 350 pc of the following second low density volume. If this matter were swept up from both sides (by the energetic events that created both cavities) to form the absorbing dust feature, the column density of the most diffuse parts of the sheet would correspond to a colour excess $E(b-y)_{\rm min} = 0\overset{\rm m}{.}061$.

In summary, the existence of the dust sheet-like feature permeating the studied area and the identical distance of the Southern Coalsack and Chamaeleon-Musca dark clouds suggest that these clouds may be dense condensations in the diffuse medium composing the sheet. Furthermore, the existence of the two low reddening volumes suggests that the sheet may be related to the interface between the Local and Loop I Bubbles.

5.1. Connection to the other data on the Local-Loop I bubble's interface

Similar effects of crossing a dust feature have been previously reported for directions lying close to the studied area. Knude (1984b) investigating the dust counterparts of arching structures towards the Sco-Cen OB association found that most stars more distant than 150 pc in SA 193 ($l = 293\overset{\circ}{.}0$, $b = 0\overset{\circ}{.}7$) clearly defined a lower envelope of $E(b-y) \approx 0\overset{\rm m}{.}020$. Such behaviour has been suggested as the effect of a spatially confined, non-coherent structure with some diffuse matter inside it.

Franco (1990) also found towards SA 195 ($l = 318\overset{\circ}{.}$, $b = -1\overset{\circ}{.}7$), SA 192 ($l = 280\overset{\circ}{.}3$, $b = -6\overset{\circ}{.}8$) and SA 175 ($l = 290\overset{\circ}{.}4$, $b = 15\overset{\circ}{.}5$), the common presence of lower envelopes with minimum colour excesses around $0\overset{\rm m}{.}050$, suggesting the existence of sheet-like features of absorbing material in front of some of the observed stars. These effects were attributed to the most diffuse parts of the interface between the Local and Loop I Bubbles, causing a minimum jump of $E(b-y) \approx 0\overset{\rm m}{.}050$, and reaching into a low density uniform volume after crossing the sheet-like structure.

Remarkably, the molecular clouds along other directions of the Sco-Cen OB association (e.g. ρ Oph, Lupus, G317-4 and R CrA) seem to define, together with Coalsack, Chamaeleon and Musca, a dense wall of matter at almost the same mean distance of 150 pc, that ranges from galactic longitudes 360° to 290° and $-25^\circ \leq b \leq 25^\circ$ (Dame et al. 1987, cf. his Fig. 7; Franco 1990). For instance, towards the ρ Oph/US-shell direction the physical relationship between the molecular complex and the edges of the neutral hydrogen shell suggested that the Ophiucus

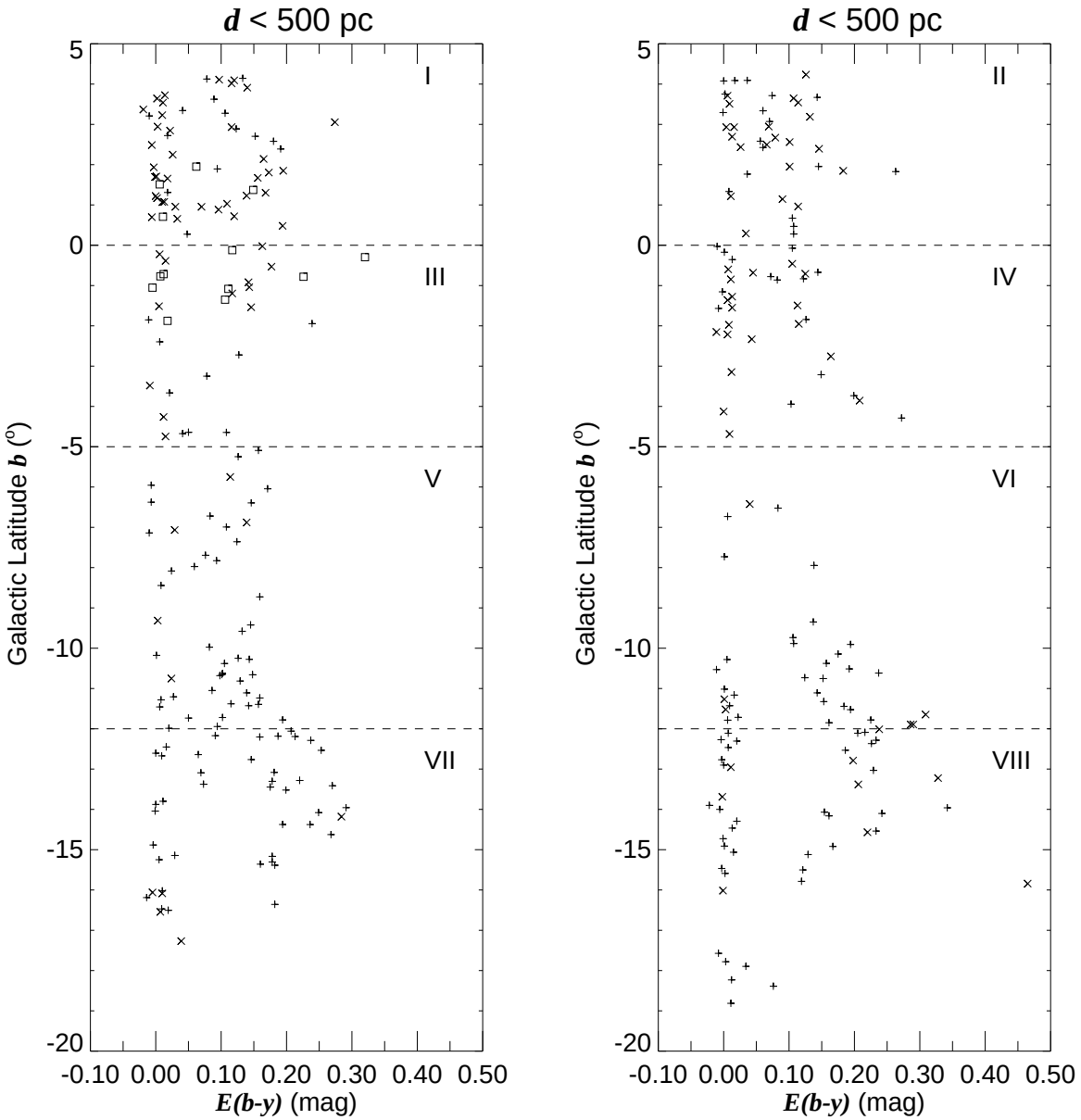

Fig. 7. b $E(b-y)$ vs. b diagrams. The extended interstellar absorbing feature, that covers the whole connecting area, causes a shift to higher values forming lower envelopes, for the non-zero reddenings, of minimum $E(b-y)$ in all eight sub-areas. The shift seems to increase with the galactic latitude (further details in the text)

complex also might have formed as condensations in the US-shell (de Geus 1992).

Moreover, the high latitude HI column density distribution of Heiles & Jenkins (1976) shows one set of arching filaments concentric to both sides of $l = 330°$, overlapping the radio continuum Loop I. These low-velocity filaments follow the flow patterns of the optical polarization vectors of Mathewson & Ford (1970), implying a direct association with the local magnetic field. Assuming that the dust producing polarization is associated to the HI gas, plots of polarization vs. distance for stars in different distance intervals suggest a distance around 115-158 pc to the HI filaments (Cleary et al. 1979). Recent polarization data of Reiz & Franco (1997) for 360 stars with accurate distance determination support this result.

The facts above lead us to the idea that Coalsack, Chamaeleon and Musca may be dense condensations superposed on the HI filaments composing the Local-Loop I Bubbles' interface, while the other mentioned clouds, ρ Oph, Lupus, G317-4, R CrA, would be at other areas of the interaction zone of the two bubbles. In this case the interstellar material might have been compressed at the far side, by the action of energetic events from OB stars of the Sco-Cen association sweeping up the unused material after the star formation, and at the near side, either by a supernova explosion occurring near the Sun, or by

what caused the local low density region. A schematic representation of this scenario would correspond to the one proposed by Iwan (1980; see his Fig. 11).

This global picture agrees with the simulations of spherical waves associated with expanding plasma bubbles by Yoshioka & Ikeuchi (1990). If at least one of the bubbles has already reached the radiative stage of evolution prior to the collision, the two interiors will not merge but a thin dense wall or diaphragm will be formed at the region of significant compression between them, and a ring-like structure of dense neutral matter will be formed at the outer rim, surrounding the wall.

Observational support for the existence of such ring-like feature has already been found on the ROSAT all-sky survey data by Egger & Aschenbach (1995). A soft X-ray shadow was discovered on the edges of the Loop I Bubble, cast by a warped annular volume of dense neutral matter that supposedly formed during the collision of the two bubbles. The shadow counterpart, a huge HI ring was also identified on the Dickey & Lockman (1990) data. The neutral hydrogen column density in some directions of the annular region jumps from less than 10^{20} to $\geq 7 \times 10^{20}$, which corresponds to the jump in colour excess caused by the dust sheet.

Egger & Aschenbach (1995) suggest that the steep increase of the column density caused by the annular feature occurs at a distance of ≈ 70 pc from the Sun. However, in the direction studied in this paper we have 65 stars before 120 pc and, for the column densities under discussion, $E(b-y)_{\rm sheet}$ is 5 times higher than $\sigma_{E(b-y)}$. These facts imply that we could easily detect the sheet at 70 pc and much probably the dust and gas wall is twisted and folded, with different directions having different distances.

6. Conclusions

The colour excesses show a possible physical association between the Southern Coalsack and the Chamaeleon-Musca dark clouds that can be summarized in the following way:

- The distribution of the colour excesses $E(b-y)$ for stars with line-of-sight *inside* and *outside* the dark clouds' contours indicates the presence of a local low absorption volume that is limited at 150 ± 30 pc from the Sun by an extended interstellar dust feature, and is followed by another region with almost no additional reddening for another 350 pc. Combined with other data on the local ISM, the existence of the dust feature permeating the whole connecting area and the identical distance of the Southern Coalsack and Chamaeleon-Musca dark clouds suggest that these clouds could be dense condensations in the diffuse medium composing the interface of the Local and Loop I Bubbles.
- Apparently, the minimum column density of the dust feature does not show a clear dependence with the galactic longitude, but may increase with the galactic latitude in the sense that $[E(b-y)_{\rm min}, b] = [0\overset{\rm m}{.}050; 0^\circ] \rightarrow [0\overset{\rm m}{.}100; -8^\circ] \rightarrow [0\overset{\rm m}{.}150; -15^\circ]$. The quoted increase suggests either the approaching of the tangential point of a warped sheet-like structure of same column density and curved away from the Sun, or an inhomogeneous sheet-like structure roughly perpendicular to the galactic plane.

Acknowledgements. The Danish Board for Astronomical Research is thanked for allocating the observing periods at the SAT, and the European Southern Observatory for the assistence during the observing runs. The Brazilian Agencies FAPEMIG and CNPq are acknowledged for supporting this research. Dr. Helge Jønch-Sørensen and the staff at the NBIfAFG are gratefully acknowledged for the invaluable help.

References

Berkhuijsen E.M., Haslam C.G.T., Salter C.J., 1971, A&A 14, 252
Bertaux J.L., Lallement R., Kurt V.G., Mironova E.N., 1985, A&A 150, 1
Blaauw A., 1964, ARA&A 2, 213
Bochkarev N.G., 1987, Ap&SS 138, 229
Bok B.J., Sim M.E., Hawaeden T.G., 1977, Nat 266, 145
Bruhweiler F.C., 1996 In: Bowyer S., Malina R.F. (eds.) Proc. IAU Colloq. 152, Astrophysics in the Extreme Ultraviolet. Kluwer, Dordrecht, p. 261
Bruhweiler F.C., Vidal-Madjar A., 1987, In: Kondo Y., et al. (eds.) Exploring the Universe with the IUE satellite, Reidel, Dordrecht, p. 467
Cederblad S., 1946, Medd. Lunds Astron. Obs. Ser. 11, 119
Cleary M.N., Heiles C., Haslam C.G.T., 1979, A&AS 36, 95
Corradi W.J.B., Franco G.A.P., 1995, A&AS 112, 95
Cox D.P., Reynolds R.J., 1987, ARA&A 25, 303
Cowie L.L., Songaila A., 1986, ARA&A 24, 499
Crawford D.L., 1975, AJ 80, 955
Crawford D.L., 1978, AJ 83, 48
Crawford D.L., 1979, AJ 84, 1858 (erratum: 85, 621)
Crawford D.L., Barnes J.V., 1970, AJ 75, 978
Crawford D.L., Mander J., 1966, AJ 71, 114
Crawford I.A., 1991, A&A 247, 183
Crutcher R.M., 1982 A&A 254, 82
Dame, T.M., Ungerechts, H., Cohen, R.S., et al., 1987 ApJ 322, 706
de Geus E.J., 1992 A&A 262, 258
Dickey J.M., Lockman F.J., 1990, ARA&A 28, 215
Egger R.J., Aschenbach B., 1995, A&A 294, L25
Feitzinger J.V., Stüwe J.A., 1984, A&AS 58, 365 (erratum: 63, 203)
Fitzgerald M.P., Stephens T.C., Witt A.N., 1976, ApJ 208, 709
Florentin Nielsen R., 1985, A 6-Channel $uvby\beta$ Spectrophotometer for the Danish 50cm Telescope, Copenhagen Univ. Obs. Internal Report 9
Franco G.A.P., 1989a, A&A 215, 119
Franco G.A.P., 1989b, A&AS 78, 105
Franco G.A.P., 1990, A&A 227, 499
Franco G.A.P., 1991, A&A 251, 581
Franco G.A.P., 1992, A&AS 93, 373
Franco G.A.P., 1995, A&AS 114, 105
Frisch P.C., 1993 Nat 364, 395
Frisch P.C., York D.G., 1983 ApJ 271, L59
Frisch P.C., York D.G., 1986 In: Smoluchowski R., Bahcall J.N., Matthews M.S. (eds.) The Galaxy and the Solar System. University of Arizona Press, Tucson, p. 83
Frisch P.C., York D.G., 1991 In: Malina R.F., Bowyer S. (eds.) Extreme Ultraviolet Astronomy. Pergamon, New York, p. 322
Frisch P.C., Welty D.E, York D.G., Fowler J.R., 1990 ApJ 357, 514
Gehrels N., Chen W., 1993 Nat 361, 706
Graham J.A., Hartigan P., 1988, AJ 95, 1197

Grasdalen G., Joyce R., Knacke R.F., Strom S.E., Strom K.M., 1975, AJ 80, 117
Grønbech B., Olsen E.H., Strömgren B., 1976, A&AS 26, 135
Hartquist, T.W., 1994, Ap&SS 216, 185
Heiles C., Jenkins E.B., 1976, A&A 46, 333
Henize K.G., 1963, AJ 68, 280
Hetem J.C.G., Sanzovo G.C., Lépine J.R.D., 1988, A&AS 76, 347
Houk N., Cowley, A.P., 1975, Univ. of Michigan Catalogue of Two-Dimensional Spectral Types for HD star, Univ. of Michigan: Ann Arbor Vol. I
Hyland A.R., Jones T.J., Mitchell R.M., 1982, MNRAS 201, 1095
Iwan D., 1980, ApJ 169, 25
Jones T.J., Hyland A.R., Harvey P.M., Wilking B.A., Joy M., 1985, AJ 90, 1191
Juda M., Bloch J.J., Edwards B.C., et al., 1991 ApJ 367, 182
Kosarev I.B., Loseva T.V., Nemtchinov I.V., Popel S.I., 1994 A&A 287, 470
Kerp J., Herbstmeier U., Mebold U., 1993 A&A 268, L21
Kholopov P.N., Samus' N.N., Frolov M.S., et al. 1985–88, General Catalogue of Variable Stars, 4th edition. Nauka Publishing House, Moscow
King D.J., Taylor K.N.R., Tritton K.P., 1979, MNRAS 188, 719
Knude J., 1978a, A&AS 33, 347
Knude J., 1978b, In: Reiz A., Andersen J. (eds.) Astronomical Papers dedicated to B. Strömgren. Copenhagen Univ. Obs., Copenhagen, p. 273
Knude J., 1979a, A&A 71, 344
Knude J., 1979b, A&A 77, 198
Knude J., 1981, A&A 97, 380
Knude J., 1983, A&A 126, 89
Knude J., 1984a In: Kondo Y., Bruhweiler F.C., Savage B.D. (eds.) Proc. IAU Colloq. 81, Local Interstellar Medium, NASA CP-2345, p. 123
Knude J., 1984b In: Proc. IAU Colloq. 81, p. 149
Knude J., 1987, A&A 171, 289
Knude J., 1991, A&A 249, 88
Lallement R., Vidal-Madjar A., Ferlet R., 1986, A&A 168, 225
Lallement R., Ferlet R., Lagrange A.M., Lemoine M., Vidal-Madjar A., 1995 A&A 304, 461
Mathewson D.S., Ford V.F., 1970, Mem. Roy. Astron. Soc. 74, 139
Malina R.F., Marshall H.L., Antia B., et al., 1994, AJ 107, 751
Müller R., 1934, Z. Astrophys. 8, 66
Nyman L.-Å., Bronfman L., Thaddeus P., 1989, A&A 216, 185
Olsen E.H., 1979, A&AS 37, 367
Olsen E.H., 1988, A&A 189, 173
Paresce F., 1984, AJ 89, 1022
Perry C.L., Johnston L., 1982, ApJS 50, 451
Reiz A., Franco G.A.P., 1997, A&AS (in preparation)
Rodgers A.W., 1960, MNRAS 120, 63
Schwartz R.D., 1991 In: Reipurth B. (ed.) ESO Scientific Report No. 11, Low Mass Star Formation in Southern Molecular Clouds, p. 93
Seidensticker K.J., 1987, Morphologie und Natur des Staubes der Dunkenlwolke *Kohlensack*. Ph. D. Dissertation, Bochum
Seidensticker K.J., Schmidt-Kaler Th., 1989, A&A 225, 192
Snowden S.L., Cox D.P., McCammon D., Sanders W.T., 1990 ApJ 354, 211
Snowden S.L., Mebold U., Hirth W., Herbstmeier U., Schmidt J.H.M.M., 1991, Sci, 252, 1529
Snowden S.L., McCammon D., Verter F., 1993, ApJ 409, L21
Snowden S.L., Freyberg M.J., Plucinsky P.P., et al., 1995, ApJ 454,643
Steenman H., Thé P.S., 1989, Ap&S 161, 99
Tapia S., 1973 In: Greenberg J.M., van de Hulst H.C. (eds.) Proc. IAU Symp. 52, Interstellar Dust and Related Topics. Reidel, Dordrecht, p. 43
Thé P.S., Wesselius P.R., Tjin A Djie H.R.E., Steenman H., 1986, A&A 155, 347
Tinbergen J., 1982, A&A 105, 53
Tobin W., 1985, A&A 142, 189
Unsöld A., 1929, Harvard Bull. 13, 870
Vaz L.P.R., Andersen J., Rabello Soares M.C.A., 1995, A&A 301, 693
Wang Q.D., Yu K.C., 1995, AJ 109, 698
Warwick R.S., Barber C.R., Hodgkin S.T., Pye J.P., 1993, MNRAS 262, 289
Weaver B., 1973, ApJ 184, 881
Weaver H., 1979 In: Burton W.B. (ed.) Proc. IAU Symp. 84, Large-Scale Characteristics of the Galaxy. Reidel, Dordrecht, p. 295
Welsh B.Y., Craig N., Vedder P.W., Vallerga J.V., 1994 ApJ 437, 638
Westerlund B., 1960, Ark. Astron. 2, 451, Uppsala Medd. 131
Whittet D.C.B., Kirrane T.M., Kilkenny D., et al., 1987, MNRAS 224, 497
Yoshioka S., Ikeuchi S., 1990, ApJ 360, 352

This article was processed by the author using Springer-Verlag LaTeX A&A style file *L-AA* version 3.